World Journal of Radiology

Submit a Manuscript: http://www.wjgnet.com/esps/
Help Desk: http://www.wjgnet.com/esps/helpdesk.aspx
DOI: 10.4329/wjr.v7.i12.459

World J Radiol 2015 December 28; 7(12): 459-474
ISSN 1949-8470 (online)

REVIEW

Multi-detector computed tomography imaging of large airway pathology: A pictorial review

Tejeshwar Singh Jugpal, Anju Garg, Gulshan Rai Sethi, Mradul Kumar Daga, Jyoti Kumar

Tejeshwar Singh Jugpal, Anju Garg, Jyoti Kumar, Department of Radiodiagnosis, Maulana Azad Medical College and associated Lok Nayak Hospital, New Delhi 110002, India

Gulshan Rai Sethi, Department of Pediatrics, Maulana Azad Medical College and associated Lok Nayak Hospital, New Delhi 110002, India

Mradul Kumar Daga, Department of Medicine, Maulana Azad Medical College and associated Lok Nayak Hospital, New Delhi 110002, India

Author contributions: Jugpal TS substantially contributed towards the conception of study and drafting the article; Garg A and Kumar J analysed the data and critically revised to assess intellectual content in the article; Sethi GR and Daga MK contributed data for study.

Conflict-of-interest statement: Authors declare no conflict of interests for this article.

Correspondence to: Jyoti Kumar, MD, Professor, Department of Radiodiagnosis, Maulana Azad Medical College and associated Lok Nayak Hospital, New Delhi 110002, India. drjyotikumar@gmail.com
Telephone: +91-99-68604361

Received: May 24, 2015
Peer-review started: May 25, 2015
First decision: August 3, 2015
Revised: October 23, 2015
Accepted: November 13, 2015
Article in press: November 17, 2015
Published online: December 28, 2015

Abstract

The tracheobronchial tree is a musculo-cartilagenous framework which acts as a conduit to aerate the lungs and consequently the entire body. A large spectrum of pathological conditions can involve the trachea and bronchial airways. These may be congenital anomalies, infections, post-intubation airway injuries, foreign body aspiration or neoplasms involving the airway. Appropriate management of airway disease requires an early and accurate diagnosis. In this pictorial essay review, we will comprehensively describe the various airway pathologies and their imaging findings by multi-detector computed tomography.

Key words: Multi detector computed tomography; Trachea; Bronchial tree; Airway abnormality; Virtual bronchoscopy

Core tip: There is a wide range of lesions affecting the airway and patients with airway pathology usually present late during the course of disease. Multi-detector computed tomography (MDCT) has become the mainstay investigation modality as it provides detailed information about the airway and its surrounding structures with high spatial resolution. Therefore it is prudent to know the various pathology affecting airway and its appearance on MDCT.

Jugpal TS, Garg A, Sethi GR, Daga MK, Kumar J. Multi-detector computed tomography imaging of large airway pathology: A pictorial review. *World J Radiol* 2015; 7(12): 459-474 Available from: URL: http://www.wjgnet.com/1949-8470/full/v7/i12/459.htm DOI: http://dx.doi.org/10.4329/wjr.v7.i12.459

INTRODUCTION

The introduction of multi-detector computed tomo-

graphy (MDCT) technology over the past decade has tremendously revolutionized imaging of airway[1,2]. Modern MDCT scanners have markedly increased the speed of data collection and cranio-caudal volume coverage enabling them to acquire thin-section, high spatial resolution images of the entire airway. These scanners can reconstruct images of varying slice thickness and in multiple planes from the acquired axial images[3-5].

The advancements in computer technology aid in processing the data sets acquired by the MDCT scanners to reconstruct the bronchial tree in three dimensions[6]. The developed computer software generates 3D view of the airway which provides clinically acceptable information with real time visualization of the entire tracheobronchial airway.

IMAGING TECHNIQUE

Thin slice axial images are acquired in a single breath hold. The imaging protocol that is used in our department for adults includes a tube voltage of 120 kV, tube current of 300 mA, 0.6 mm × 128 slices, a pitch of 1.5 with a matrix size of 512 × 512. For children, the tube voltage is reduced to 80 kV and tube current is altered to 110 mA.

Administration of contrast is generally not required for assessment of airway. However it is used in suspected cases of extraluminal compressive lesions to delineate the various mediastinal vascular structures and for suspected neoplastic etiology. Non-ionic iodinated contrast medium may be given using a dose of 1 mL/kg for adults and 1.5 mL/kg for children through peripheral venous access route.

Image reconstruction

The cross-sectional images are then transferred to a separate graphic computer. Reconstruction is done using standard visualization software. The acquired near isotropic data is used to generate multiplanar reformations (MPRs), minimum intensity projections (MinIPs) and volume rendered images for 3D reconstruction.

Two basic methods of 3D imaging are currently employed in airway reconstruction including external rendering and internal rendering. The external rendering of the airway shows its external surface and is also called computed tomography (CT) tracheobronchography. Internal rendering or virtual bronchoscopy (VB) allows navigation through the internal airway lumen of airway using the "fly through" virtual endoscopy CT software. The airway reconstructed by VB closely resemble those seen on conventional bronchoscopy[7-9]. However, VB can evaluate the airway distal to a high grade stenosis which is not possible on fiberoptic bronchoscopy.

NORMAL ANATOMY

Trachea

Trachea is a tubular structure extending from the level of the cricoid cartilage (6th cervical vertebral level) to the carina (5th thoracic vertebral level). Trachea is made up of multiple C shaped cartilages[10]. It measures 10 to 11 cm in length[10]. The trachea is divided into extra- and intra-thoracic parts. The extrathoracic part extends from the level of inferior border of cricoid upto the thoracic inlet. The intrathoracic portion extends from the thoracic inlet to the carina.The normal tracheal diameter in men ranges from 13 to 25 mm in the coronal dimension and 13 to 27 mm in the sagittal dimension[11,12]. In women, trachea is smaller and its dimension range from 10 to 21 mm in the coronal plane and 10 to 23 mm in the sagittal plane[11,12]. The posterior portion of the tracheal wall, lying between the open ends of the tracheal cartilages, is a thin fibromuscular membrane termed the posterior tracheal membrane. The cross section of trachea has marked variability in appearance, which may appear round, oval or horse shoe shaped. The posterior tracheal membrane may appear convex posteriorly, flat or convex anteriorly.

Carina

Trachea divides at the level of sternal angle (4th-5th dorsal vertebral levels) at the carina into the right and left mainstem bronchi[11]. The normal carinal angle ranges between 70°-100°.

Mainstem, lobar and segmental bronchi

The mainstem bronchi extend infero-laterally from the carina into the pulmonary hila. At the pulmonary hila, they branch further to form the bronchial tree within the pulmonary parenchyma. The mainstem bronchi divide into lobar bronchi. There are 3 lobar bronchi on rigth side and 2 on left side. The lobar bronchi further divides into segmental and subsegmental bronchi. There are approximately 23 generations of branching till the bronchi form the alveoli[13]. The segmental bronchi are accompanied by segmental arteries that form a broncho-pulmonary segment.

The bronchi on MDCT appear as small circular lucencies on axial scans. Bronchi that course obliquely to the axial plane are more difficult to evaluate on axial scans and therefore require MPRs images and MinIP images (Figure 1). VB also provides the intraluminal view (Figure 2).

PATHOLOGY

The pathological conditions affecting airway vary from innocuous to sinister. To add to the diagnostic dilemma, identification of tracheal disease is notoriously difficult. Patients become symptomatic very late in the natural history of diseases affecting the airway. Patients with tracheobronchial pathology can present with breathlessness, persistent cough, stridor, recurrent cyanotic episodes and haemoptysis in varying severity, depending upon the degree of airway involvement. These may cause sudden deterioration of the patient's clinical condition. Therefore rapid and accurate diagnosis is imperative to reduce morbidity and mortality.

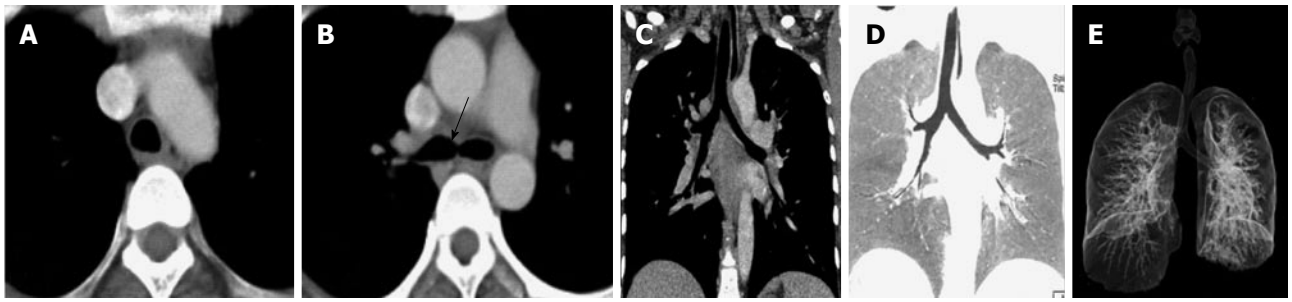

Figure 1 Normal arway. Axial image at the level of arch of aorta (A) shows a typical inverted U shaped trachea with thin fibromuscular membrane in posterior portion lying between open ends of tracheal cartilages. Axial image (B) at the level of carina (arrow) shows dichotomous branching of trachea at its distal end into right and left main bronchi. Coronal MPR image (C) shows trachea and mainstem bronchi as uniform tubular structures in midline within the mediastinum. Coronal reconstructed MinIP image (D) shows trachea and its bronchial branches as tubular air containing structures continuous from thoracic inlet till its divisions into the lung parenchyma. Volume rendered image (E) is the external rendered image showing 3-dimensional display of external surface of the airway and lung parenchyma. MPR: Multiplanar reformation; MinIP: Minimum intensity projection.

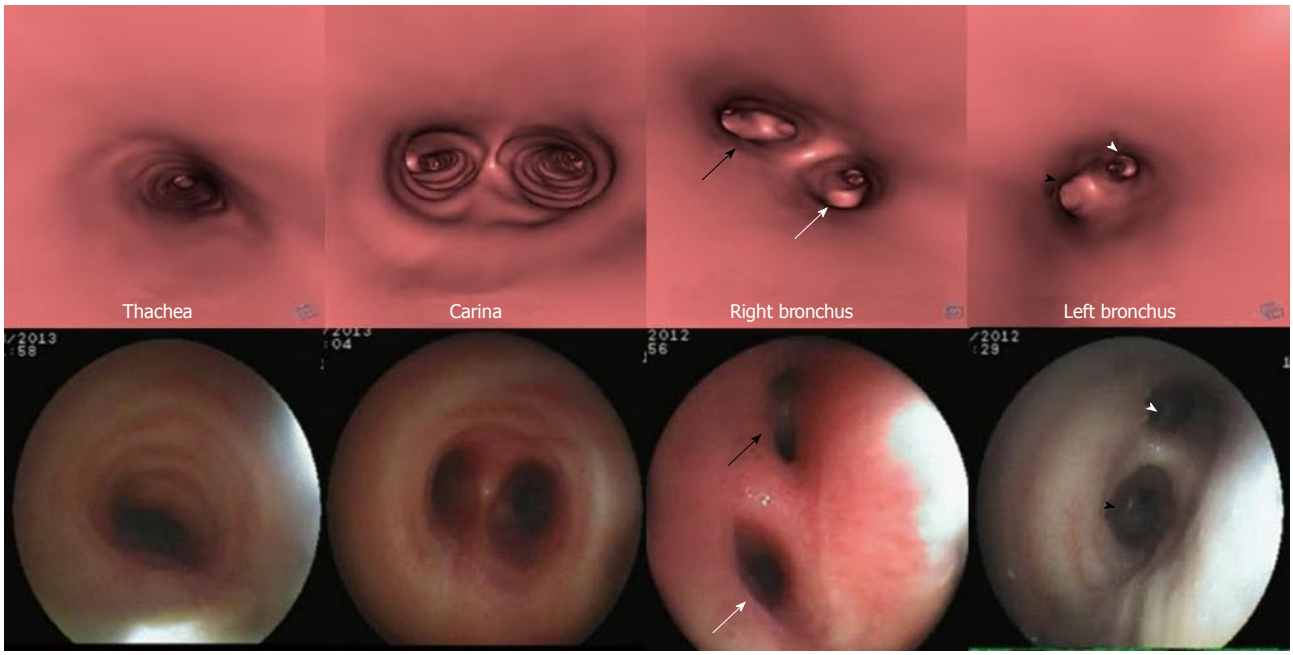

Figure 2 Virtual bronchoscopy of normal airway. Virtual bronchoscopy or internal rendered images reconstructed using dedicated "fly through" software at the level of trachea, carina, right and left main bronchus (top row) with corresponding appearance on fiberoptic bronchoscopy (bottom row). The division of right bronchus into upper lobe (white arrow) and bronchus intermedius (black arrow) and division of left main bronchus into upper (black arrowhead) and lower lobe bronchus (white arrowhead) is seen.

For descriptive purposes, the lesions affecting airway may be broadly classified as focal and diffuse lesions[14]. A lesion is characterized as focal when it affects a single short segment of airway, whereas it is characterized as diffuse if it involves either long segment of airway or when multiple lesions are detected.

FOCAL AIRWAY LESIONS

Intrinsic focal lesions

Tracheobronchial neoplasm: Tracheobronchial neoplasm is one of the commonest focal lesion involving the airway[15]. Tracheobronchial involvement by a malignant process can be both primary and secondary. Mostly airway is secondarily invaded by primary neoplasms arising from adjacent organs. Trachea is in close approximation with various organs in its extrathoracic and intrathoracic course. Therefore primary malignancy of adjacent organs like lung, esophagus or thyroid can invade the tracheobronchial tree.

Primary lung carcinoma is a disease with a very high mortality rate worldwide and commonly involves the airway. The main histopathological types include: adenocarcinoma, squamous cell carcinoma (SCC), small cell carcinoma and large cell carcinoma of which SCC and small cell carcinoma are most common types originating from the central airway[16,17]. SCC has an intraluminal growth pattern that can cause airway obstruction leading to pulmonary atelectasis or lobar collapse (Figure 3)[16]. Bronchial obstruction is much less common with small cell carcinoma than with SCC. The most common imaging finding seen in small cell

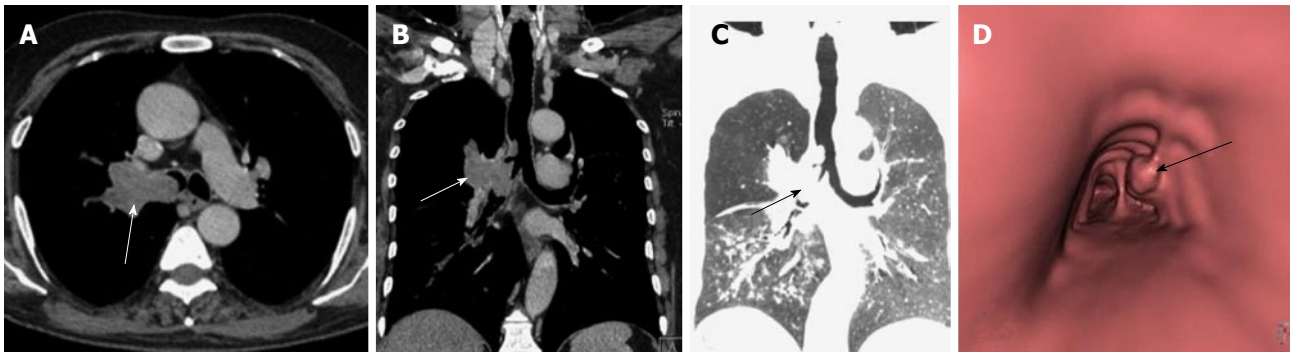

Figure 3 Squamous cell lung carcinoma. Contrast enhanced axial (A) and coronal MPR (B) images show enhancing soft tissue mass in right perihilar region with intraluminal extension of growth into the right mainstem bronchus and lower trachea (arrow). Coronal MinIP image (C) shows attenuation of right mainstem bronchus with a polypoidal growth extending into lower trachea (arrow). Virtual bronchoscopy (D) shows an irregular polypoidal intraluminal mass in lower trachea (arrow). MPR: Multiplanar reformation; MinIP: Minimum intensity projection.

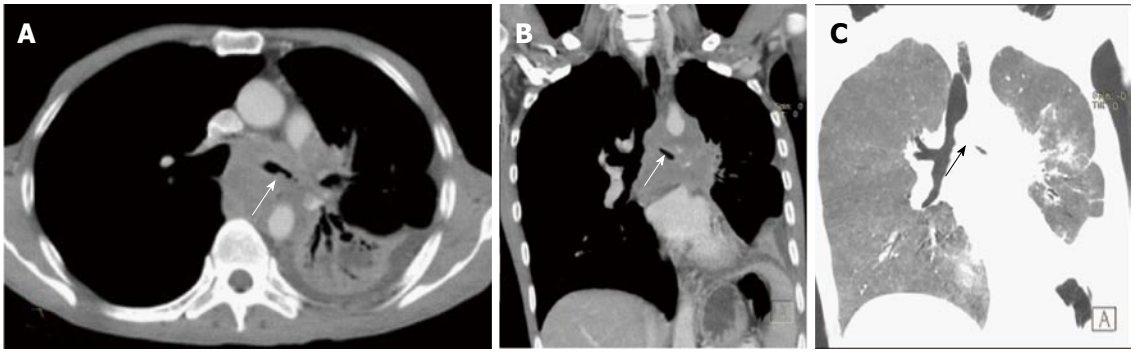

Figure 4 Small cell lung cancer. Axial (A) and coronal MPR (B) images show heterogeneously enhancing mass lesion encasing and attenuating left main bronchus and its lower division with mediastinal invasion and associated collapse-consolidation of left lower lobe. Coronal MinIP image (C) shows attenuated left main bronchus (arrow). MPR: Multiplanar reformation; MinIP: Minimum intensity projection.

carcinoma is that of extensive hilar or mediastinal lymphadenopathy (Figure 4)[18].

Primary tracheal neoplasm can also occur but are very rare. Majority of the primary tracheal neoplasms in adults are malignant with common histopathological patterns comprising of SCC, adenoid cystic carcinoma, carcinoid, mucoepidermoid carcinoma, and papilloma. SCC is the most common tracheal tumor and is more common in men[19]. It is highly associated with cigarette smoking and is histologically identical to lung SCC[14]. SCC appears as a polypoid intraluminal lesion generally in the lower third of trachea. It typically has irregular margins as it arises from the surface epithelium. It may invade mediastinum by direct extension or lymphatic spread (Figure 5)[20]. The second common cell type is adenoid cystic carcinoma (ACC) which occurs in younger patients with equal sex distribution. ACC arises within the submucosal glands and therefore has a smooth outline (Figure 6)[21]. The mucosal covering of the lesion rarely ulcerates in contrast to SCC. Lymphadenopathy and metastases are also uncommon[22].

Benign tumors of the airway include endobronchial carcinoid, hamartoma and papillomas. Endobronchial carcinoids are the most common airway tumors in adolescents and young adults. They generally arise within the central bronchi causing cough, hemoptysis, and airway obstruction[23]. They appear as an intensely enhancing endobronchial or hilar masses with post obstructive features like atelectasis or air trapping[23]. About one-fourth of these tumors can also show calcification on CT[24].

Respiratory papilloma is caused by human papilloma virus infection of the upper airway. The infection is usually acquired during birth or rarely through oro-genital sexual route. The tracheo-laryngeal form of papilloma is the commonest form and occurs in 2%-17% cases[25]. Respiratory papilloma is a benign endoluminal lesion that commonly involves larynx, trachea and the mainstem bronchi. It is a well circumscribed polypoid lesion which does not extend across the wall of trachea or bronchi (Figure 7)[25]. Respiratory papillomas can occur at multiple sites along the airway. VB can show the entire extent of the disease without the risk of downstream spread, which can be a problem with conventional bronchoscopy. Papillomas can cause airway obstruction and lead to post obstructive changes like atelectasis, pneumonia or pneumothorax. The most serious long term complication is malignant degeneration of papilloma to SCC[26].

MDCT acquired after contrast administration is currently the standard imaging modality to diagnose and stage central airway tumors. Axial images along

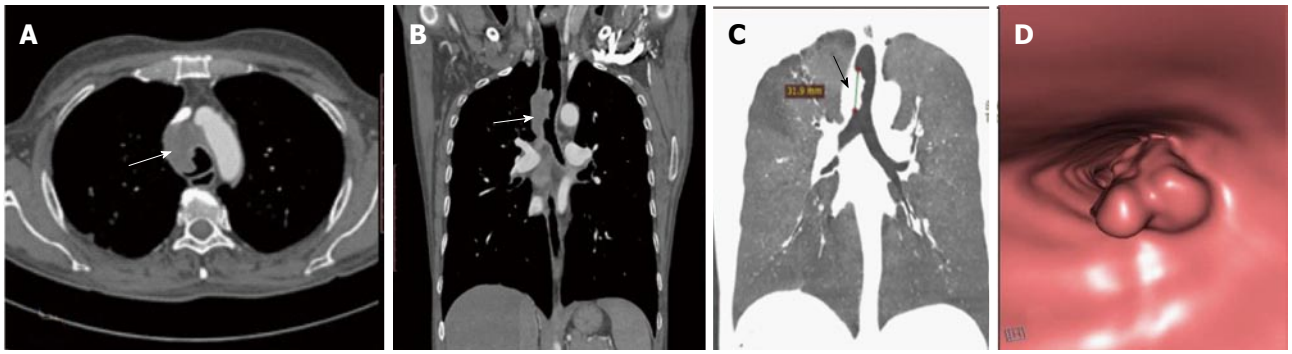

Figure 5 Squamous cell carcinoma of trachea. Axial (A) and coronal MPR (B) images show eccentric soft tissue mass with irregular surface involving trachea (arrow in B) with mediastinal extension (arrow in A). Coronal MinIP (C) shows partial attenuation of mid tracheal lumen involving a length of 3.19 cm (arrow). Virtual bronchoscopy (D) shows this mass lesion as irregular intraluminal growth along the right wall of trachea causing tracheal luminal narrowing. MPR: Multiplanar reformation; MinIP: Minimum intensity projection.

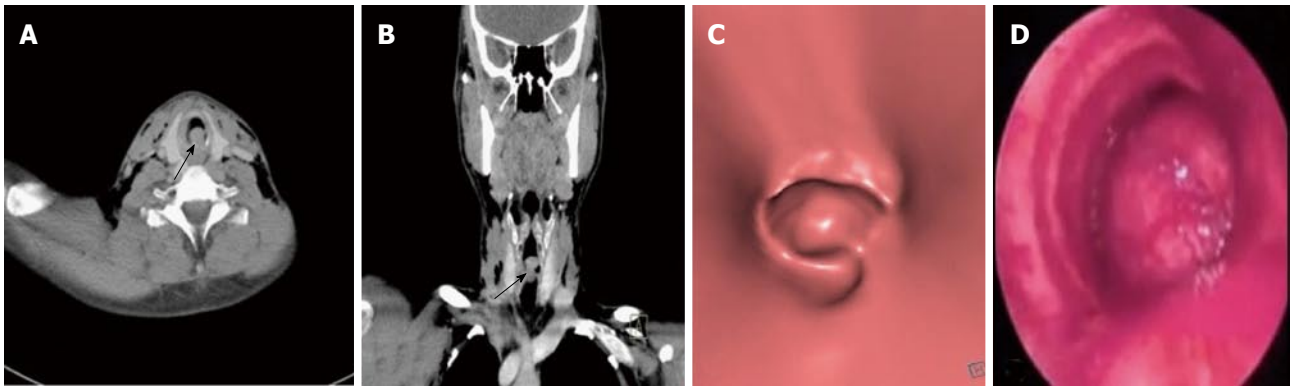

Figure 6 Adenoid cystic carcinoma of trachea. Axial (A) and coronal MPR (B) images show polypoidal mass with smooth outline within the trachea in subglottic region causing near complete attenuation of the airway (arrow). Virtual bronchoscopy (C) shows intraluminal smooth mass within trachea similar to that seen on conventional bronchoscopy (D). MPR: Multiplanar reformation.

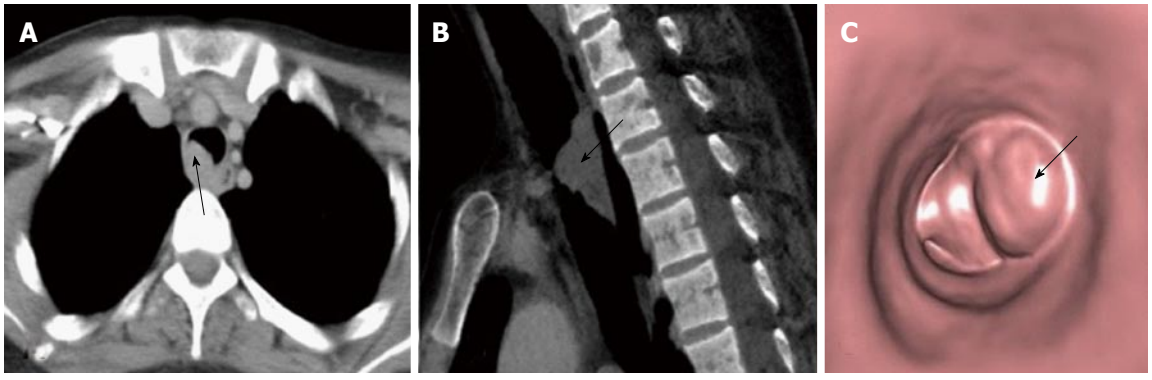

Figure 7 Respiratory papilloma. Axial (A) and sagittal MPR (B) images show a smooth polypoidal soft tissue mass arising from the postero-lateral wall of trachea (arrow). Virtual bronchoscopy (C) shows the intraluminal mass lesion with smooth surface (arrow). MPR: Multiplanar reformation.

with reconstructed MPR and 3D images provide comprehensive information about the involvement of airway by the tumor and its relationship with adjacent structures. MDCT can also detect associated lymph nodal spread and metastases (both intra-pulmonary and distant sites), thereby altering tumor staging. VB images provide an intraluminal view of the tumor involving the airway. These also score over conventional bronchoscopy due to their inability to evaluate the airway distal to a high grade narrowing or complete obstruction. This can have a significant impact on patient management as palliative stent placement in the airway can be offered to patients with proximal occlusive lesion and patent distal airway.

Post tracheostomy complications: Prolonged tracheal intubation and tracheostomy can cause airway complications. Tracheal stenosis is a frequently encoun-

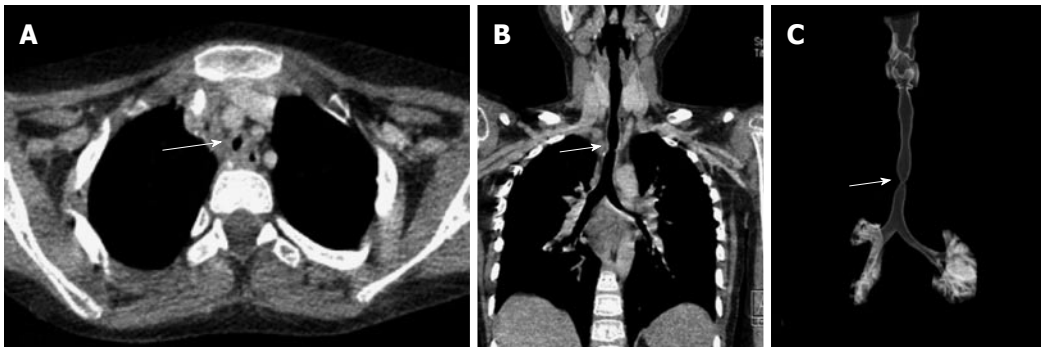

Figure 8 Post intubation tracheal stenosis. Axial (A), coronal MPR (B) and VRT (C) images show a focal short segment concentric narrowing of tracheal lumen giving an "hourglass" configuration better appreciated on coronal images. MPR: Multiplanar reformation; VRT: Volume rendering technique.

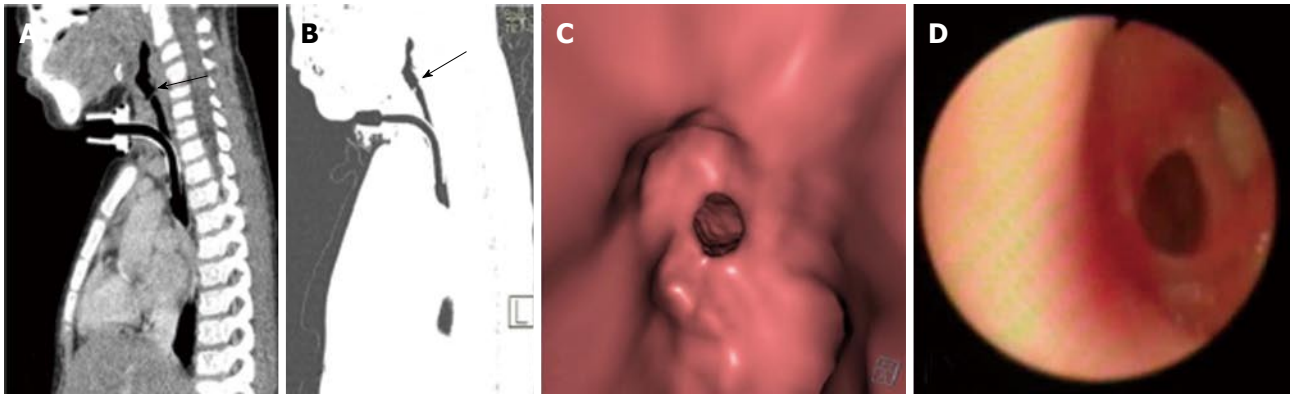

Figure 9 Tracheal membrane. Sagittal MPR (A) and sagittal MinIP (B) images show a partially occluding thin membrane in subglottic airway (arrow). Note made of tracheostomy tube insitu. Virtual bronchoscopy (C) shows circumferential membrane causing narrowing of airway lumen with similar finding confirmed on fiberoptic bronchoscopy. MPR: Multiplanar reformation; MinIP: Minimum intensity projection.

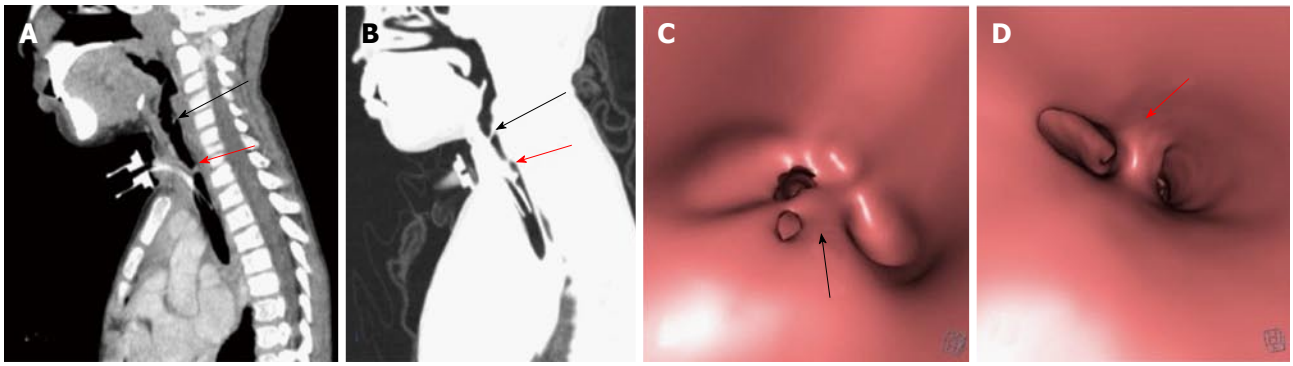

Figure 10 Post intubation mucosal synechiae. Sagittal MPR (A) and MinIP (B) images show thin membrane like adhesions within the airway at subglottic (black arrow) and upper tracheal (red arrow) levels extending across the airway lumen and compromising its patency suggestive of synechiae formation. The corresponding appearance of these synechiae are very well demonstrated on virtual bronchoscopy (C and D). MPR: Multiplanar reformation; MinIP: Minimum intensity projection.

tered entity in these patients. The stenosis generally occur at two sites: At the level of endotracheal tube cuff which is most common site and at the stoma site. The high pressure of the endotracheal tube balloon causes mucosal injury of tracheal wall. This leads to tissue scarring and ultimately tracheal stenosis.

The most common CT finding in post intubation stenosis is a localized area of narrowing of tracheal lumen[27,28]. This focal circumferential narrowing generally produces a characteristic hourglass configuration (Figure 8). Less common findings include a thin membrane projecting into the tracheal lumen (Figure 9). Due to mucosal injury there can also be formation of multiple mucosal synechiae compromising the tracheal lumen (Figure 10).

MDCT with multi planar reformats and VB provides information regarding the stenosis, *i.e.*, grade of stenosis, distance of stenotic segment from the vocal cord and length of the stenotic segment. These findings give a detailed road map to the surgeons before the

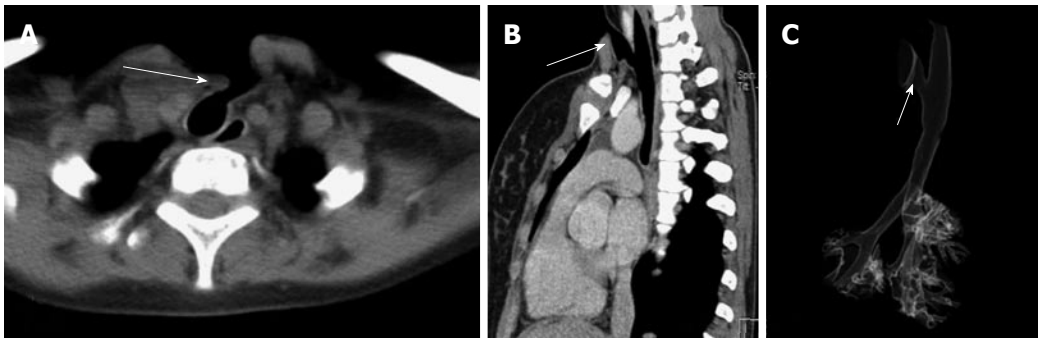

Figure 11 Post tracheostomy tracheo-cutaneous fistula. Axial (A) and oblique sagittal MPR (B) images show the fistula as an abnormal tract extending from antero-lateral wall of upper trachea to the skin surface (arrow). This fistulous tract is very well demonstrated on VRT image (C, arrow). MPR: Multiplanar reformation; VRT: Volume rendering technique.

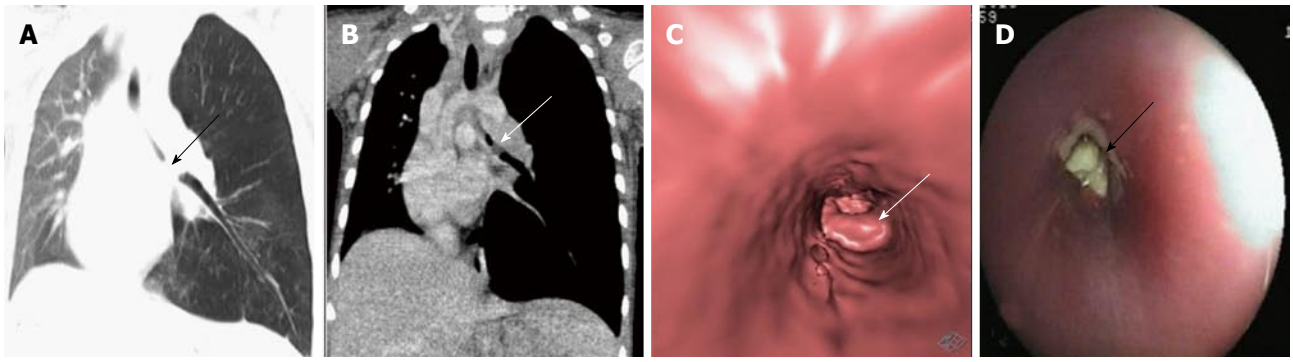

Figure 12 Foreign body aspiration. Coronal MPR images of thorax in lung settings (A) and mediastinal window settings (B) reveal soft tissue density attenuating left main bronchus (arrow) with associated hyperinflation of left lung. Virtual bronchoscopy (C) shows obstruction of left main bronchus with lobulated surface confirmed to be endobronchial foreign body (arrow) on conventional bronchoscopy (D). MPR: Multiplanar reformation.

patient is taken up for surgery. The MPR and volume rendering technique images are helpful in appreciating the vertical length of the lesion more precisely.

Other complication like diverticulum at the stoma site and tracheocutaneous fistula can also develop after tracheostomy. MDCT can accurately demonstrate the location, dimension and tract of the fistula which has an implication on the surgical management of these patients (Figure 11).

Foreign body aspiration: Foreign body aspiration is generally encountered in young children (aged between 6 mo to 5 years) and is a frequent cause of morbidity and mortality[29,30]. Foreign body aspiration is potentially life threatening if not recognised early and appropriately treated. Any child with acute stridor should always be evaluated for potential aspiration of foreign body. However, patients with chronically impacted foreign body are difficult to diagnose. They usually present with recurrent wheezing and radiographs if obtained may show pulmonary infiltrates, bronchiectatic changes or lung abscess[31]. Aspiration of organic vegetative objects is more dangerous as these swell with bronchial secretions and cause progressively increasing airway obstruction. Allergic and chemical bronchitis is also a frequent complication of aspiration of organic foreign body[32].

In suspected cases of foreign body aspiration, obtaining radiographs in both inspiratory and expiratory phases can be helpful. Decubitus view and fluoroscopic assessment can also be performed to look for features of airway obstruction like hyperinflation. However, radiographs are normal in around one-third of these cases and nearly 90% of these foreign bodies are radiolucent[33]. Therefore, the advantage of MDCT in evaluating these cases lies in the fact that it can detect both radioopaque and radiolucent foreign bodies (like plastic and organic food items). The aspirated radiolucent objects usually appear as non-enhancing soft tissue structure within the airway causing partial or complete airway obstruction (Figure 12). CT also help in identifying ancillary post obstructive findings like hyperinflation, lobar atelectasis or complete lung collapse (Figure 13)[34].

Broncholithiasis: The presence of calcific/ossific material within the bronchial lumen is called broncholithiasis. It is most commonly associated with erosion of the airway by a calcified lymph node caused by long-standing foci of granulomatous lymphadenitis like tubercular infection which can then extrude into the lumen of the bronchus. Other rarer causes include *in-situ* calcification of chronically aspirated foreign body

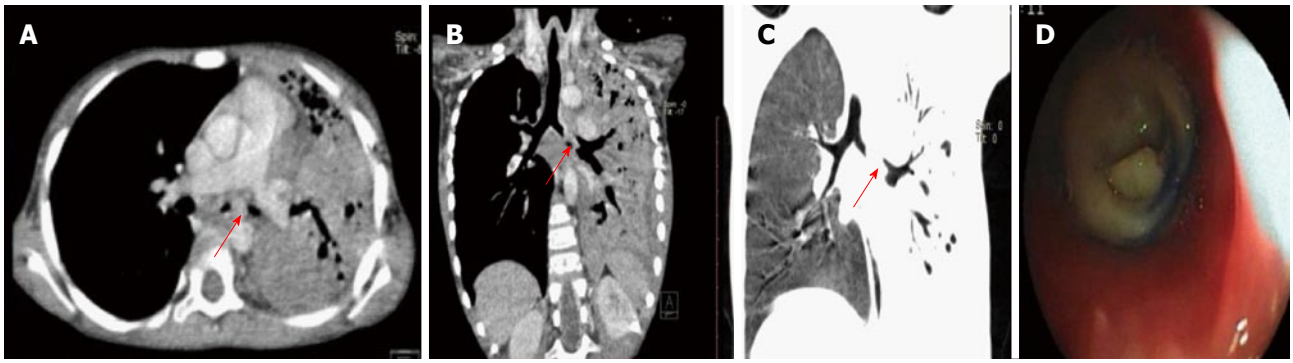

Figure 13 Chronic foreign body aspiration. Axial (A) and oblique coronal MPR (B) images reveal soft tissue density partially occluding the left main bronchus (arrow) with consolidation of left lung and associated bronchiectatic changes. Coronal MinIP image (C) shows attenuation of left main bronchus (arrow) with collapse of left lung. Endobronchial foreign body within left main bronchus was confirmed to be a small piece of plastic on conventional bronchoscopy (D). MPR: Multiplanar reformation; MinIP: Minimum intensity projection.

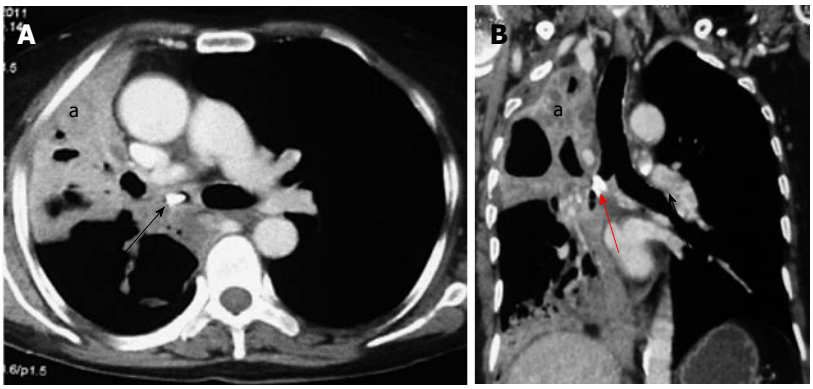

Figure 14 Broncholith. Axial (A) and coronal MPR (B) images show a hyperdense calcific density within the right main bronchus (arrow) with collapse-consolidation and bronchiectasis in the right lung (a). MPR: multiplanar reformation.

or even migration of calcified pleural plaque into the bronchus[35]. CT has high spatial resolution and superior ability to depict calcification. Therefore it provides useful information in the evaluation of suspected case of broncholithiasis. The presence of endobronchial or peribronchial calcified nodule is highly suggestive of broncholithiasis. It can also show features of bronchial obstruction like atelectasis, obstructive pneumonitis or bronchiectasis (Figure 14).

Tracheal wall pathology

Post traumatic tracheal rent: Tracheo-bronchial injuries are rare but they can occur in motor-vehicle accidents with trauma to the thoracic cavity. The injury predominantly involves the posterior membranous wall of intrathoracic trachea. The injury occurs due to sudden increase in the intra-airway pressure against a closed glottis at the time of injury[36].

MDCT depicts the site of injury as a focal or circumferential defect in tracheal wall, deformed tracheal contour or fistulous communication with adjacent structures (Figure 15)[36]. Other non-specific signs include pneumo-mediastinum, pneumo-thorax and non-resolving subcutaneous emphysema. Tracheo-bronchial injury is an emergency and early diagnosis with immediate surgical repair is necessary to reduce morbidity and mortality in such patients.

Tracheo-esophageal fistula: Esophageal atresia and tracheoesophageal fistula are a group of congenital anomalies involving the structures arising from primitive foregut. They occur due to an unknown intrauterine insult during the normal process of separation of primitive foregut into trachea and esophagus. (Figure 15)[37]. Tracheo-esophageal fistula can be an isolated anomaly or a part of VACTERL complex (vertebral, anal, cardiac, tracheal, esophageal, renal, and limb anomalies)[38].

However current usefulness of pre-operative CT in cases of tracheoesophageal fistula is controversial. It provides limited information about the fistulous tract as compared to endoscopy. Thus, the use of CT scan is not routinely recommended in the management of tracheoesophageal atresia.

Extrinsic focal lesions

Vascular compression: Anomalous mediastinal vessels (aorta and pulmonary arteries) are important causes of compression of the trachea. Although a majority of these patients are asymptomatic, vascular

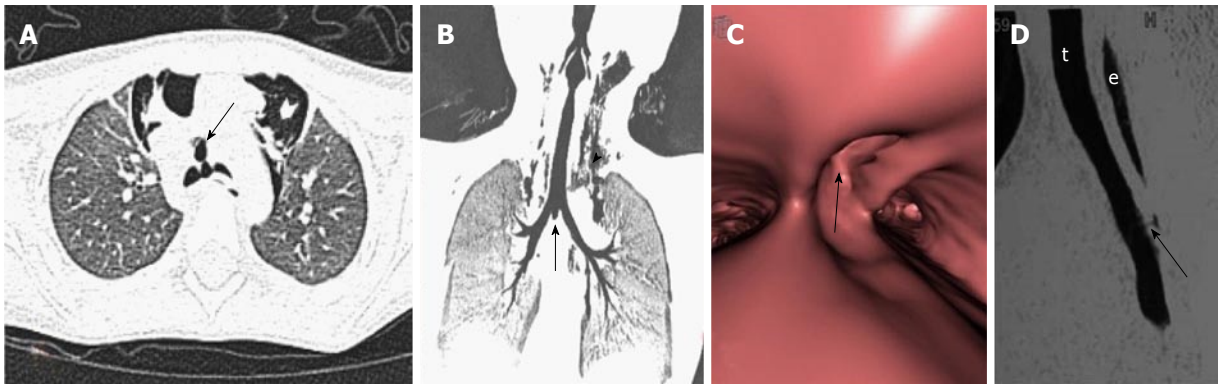

Figure 15 Airway wall pathology. Traumatic tracheal rent-Axial (A) and oblique coronal MinIP (B) images show a focal air containing outpouching at the level of carina in midline projecting antero-inferiorly (arrows). Virtual bronchoscopy (C) shows a focal defect within the wall of trachea at the level of carina (arrow). Note made of marked subcutaneous emphysema (arrowhead in B). Tracheo-esophageal fistula-sagittal MPR image (D) of another case shows a thin faint air containing tract (arrow) extending from esophagus (e) to trachea (t). MPR: Multiplanar reformation; MinIP: Minimum intensity projection.

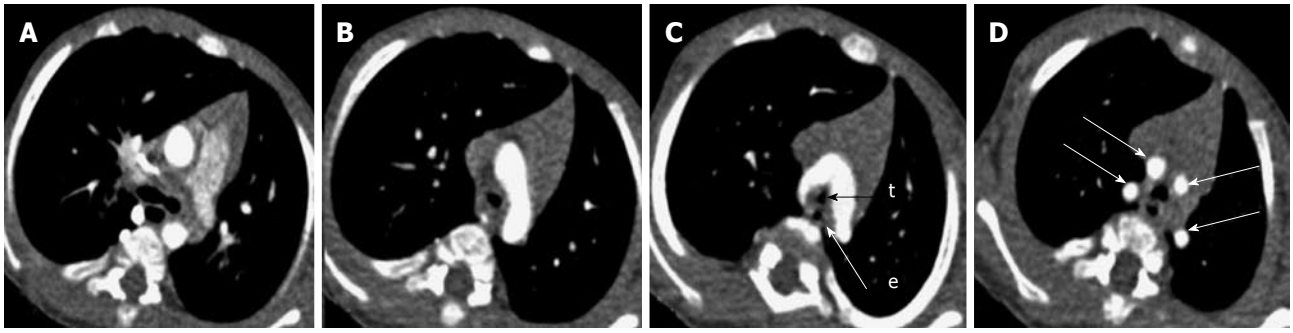

Figure 16 Double aortic arch. Serial axial images (A-D) of thorax (in caudo-cranial direction) reveal 2 aortic arches encircling and compressing trachea (t) and esophagus (e). Ipsilateral subclavian and common carotid arteries arise from each arch giving a characteristic "4-vessel sign" (arrows in D).

compression of the airway have been observed in 13%-26% of children who undergo bronchoscopy for persistent wheezing, stridor and apnea[39]. The vascular anomalies that present with airway compression include double aortic arch, anomalous course of innominate artery and pulmonary artery sling.

Double aortic arch is a vascular anomaly that occurs due to non regression of right aortic arch during intrauterine development. There is persistence of both right and left aortic arches, which form a vascular ring encircling and compressing esophagus and trachea. Each arch gives off two branches - the common carotid and subclavian arteries supplying ipsilateral sides of the body giving the characteristic "four vessel sign" (Figure 16). In most of the cases the right sided arch is higher and is larger in diameter. However they can also be in the same plane or the right sided arch may even be lower in location. Sometimes one of the arches may be replaced by a fibrous cord with absent luminal patency[40].

The innominate artery can sometimes have an anomalous course and originate at a point farther along the arch than is normal; when it does so, it winds around the anterior surface of the trachea as it courses upward and to the right. If this vessel is large and taut, it can compress the trachea to a serious degree (Figure 17).

Left pulmonary artery sling is a rare anomaly characterized by abnormal origin and course of left pulmonary artery. The left pulmonary artery has an anomalous origin from right pulmonary artery and courses between trachea and esophagus before entering the left hilum (Figure 18). It is thought to result from a failure of formation of the 6th aortic arch. Nearly half of the infants born with this condition present with symptoms of airway compression at birth. At one month of age, approximately 65% of the children develop stridor of varying degree[41].

Bronchogenic cyst: Bronchogenic cysts are intra-thoracic cystic developmental lesions caused by abnormal antenatal budding of the tracheobronchial tree[42,43]. These are included under the broad spectrum of foregut duplication cysts that also includes neuren-teric cysts and enteric cysts. Bronchogenic cysts are typically located in the middle mediastinum with subcarinal region being the most common site followed by right paratracheal location[44]. Rarely, they can also occur as intra-pulmonary lesions most of which are located in the lower lobes[44]. Small bronchogenic cysts are usually asymptomatic; however large lesions can cause mass effect on adjacent structures like the airway

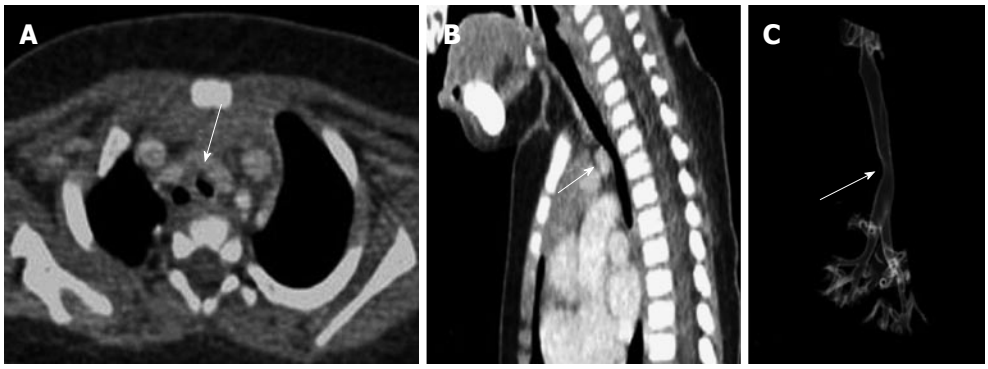

Figure 17 Innominate artery compression. Contrast enhanced axial (A) and sagittal MPR (B) images show extraluminal compression of trachea by anomalous course of innominate artery winding around the anterior wall of trachea (arrow). 3D VRT image (C) shows smooth indentation on the tracheal air column (arrow). MPR: Multiplanar reformation; VRT: Volume rendering technique.

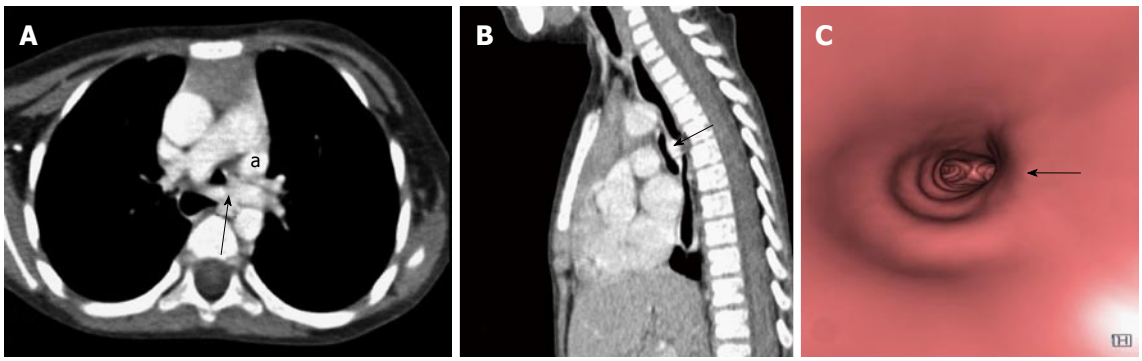

Figure 18 Left pulmonary artery sling. Contrast enhanced axial (A) and sagittal MPR (B) images reveal aberrant course of left pulmonary artery between trachea and esophagus (arrow) causing tracheal compression and vascular indentation on esophagus. Note made of left superior vena cava (a). Virtual bronchoscopy (C) shows an eccentric impression causing focal narrowing of the tracheal lumen (arrow). MPR: Multiplanar reformation.

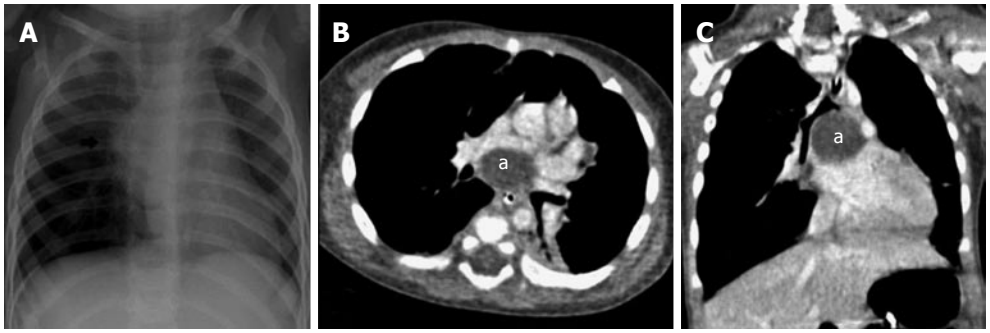

Figure 19 Subcarinal bronchogenic cyst. Frontal radiograph of chest (A) reveals mediastinal widening (arrow). Contrast enhanced axial (B) and coronal MPR (C) images reveal well defined non-enhancing homogenous fluid attenuation lesion in subcarinal location (a) narrowing the bronchial divisions with resultant subsegmental atelectasis in left lower lobe. MPR: Multiplanar reformation.

or esophagus causing respiratory distress and feeding difficulty respectively[43,44].

Bronchogenic cysts are usually single and show characteristic MDCT appearance of a well-circumscribed round or oval lesion with homogenous fluid attenuation (Figures 19 and 20). On contrast administration, they usually do not enhance or show minimal peripheral rim enhancement. The presence of thick walls, solid component, calcification or septations is unusual. If they cause substantial mass effect on adjacent airways post obstructive features like hyperinflation or lung collapse may also occur. Bronchogenic cysts can sometimes appear as an air containing cystic lesion if a fistulous communication develop with the airway (Figure 21).

Impacted esophageal foreign body: Foreign body ingestion with impaction within the oesophagus can rarely cause compression on the airway. Such cases are rarely encountered however may be seen especially in very young children who have a compliant airway which gets compressed extraluminally leading to airway compromise and post obstructive pulmonary changes

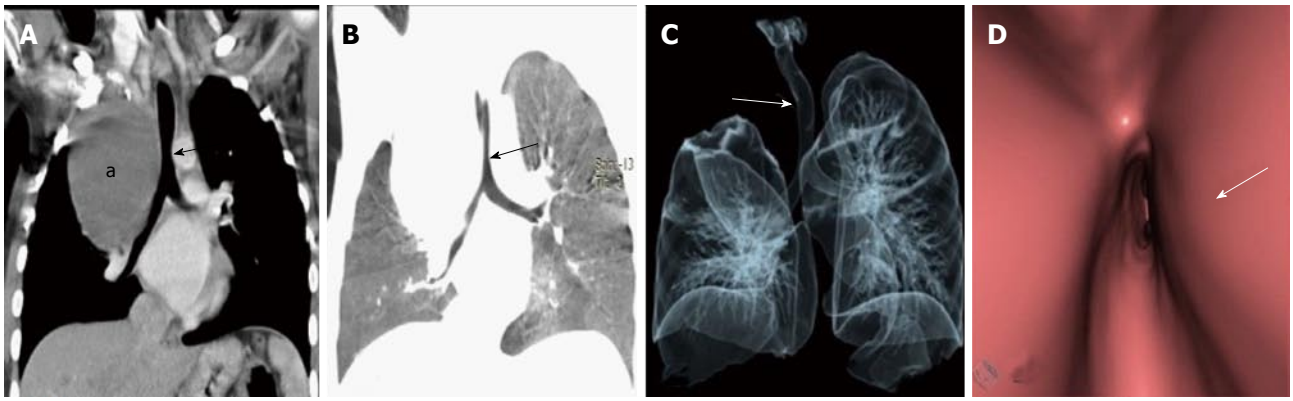

Figure 20 Paratracheal bronchogenic cyst. Coronal MPR image (A) shows large well defined non enhancing fluid attenuation lesion (a) in right paratracheal location with mass effect on adjacent trachea causing tracheal luminal attenuation (arrow). Coronal MinIP (B) and VRT (C) images show extrinsic mass effect on the airway (arrow) and right lung. Virtual bronchoscopy (D) clearly demonstrates the smooth extraluminal compression along the right wall of trachea causing luminal compromise. MPR: multiplanar reformation; MinIP: Minimum intensity projection; VRT: Volume rendering technique.

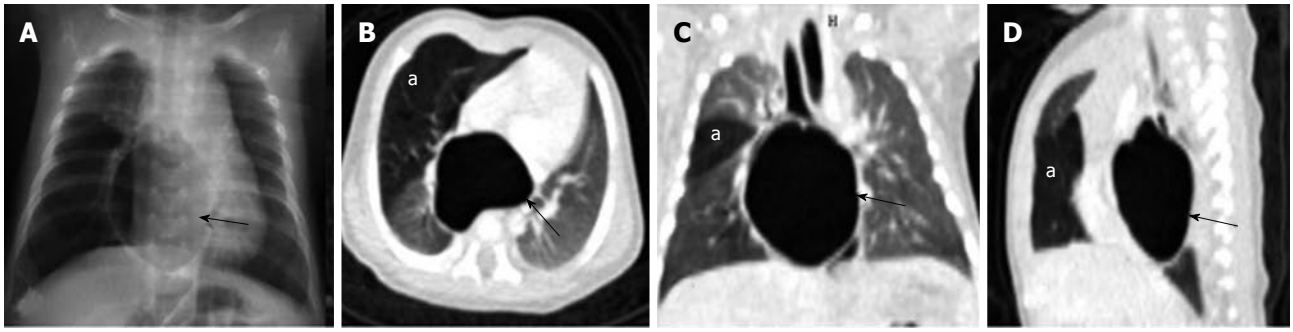

Figure 21 Bronchogenic cyst. Frontal radiograph of chest (A) shows a well-defined air filled cystic lesion in the retrocardiac location. Axial (B), coronal (C) and sagittal (D) MPR images show a large well defined homogenous air containing lesion (arrow) with carinal widening. The lesion is causing partial airway obstruction seen as air trapping in right middle lobe (a). MPR: Multiplanar reformation.

like atelectasis, consolidation and collapse (Figure 22)[45,46].

Lymphadenopathy: The mediastinum and pulmonary hila have a rich network of lymphatic tissues. These can enlarge due to various disease conditions including infective aetiologies like tuberculosis, histoplasmosis and malignant conditions like lymphoma and small cell lung cancer[47]. These may obstruct the airway to cause post obstructive pulmonary changes like atelectasis and collapse (Figure 23). Enlarged lymph nodes may also erode and infiltrate into the adjacent tracheal and bronchial wall leading to focal discontinuity of the airway wall (Figure 24). MDCT clearly depicts the cause of compression as enlarged lymph nodes and may also characterize primary pathology leading to lymphadenopathy.

DIFFUSE AIRWAY LESIONS

Saber-sheath trachea

Saber-sheath trachea is an abnormal morphological appearance of trachea seen in association with chronic obstructive pulmonary disease (COPD). It is seen almost exclusively in men and is characterized by reduced transverse and increased sagittal diameter of intrathoracic trachea (Figure 25). The sagittal-to-coronal diameter ratio is greater than 2[48]. The extra-thoracic trachea is not affected. Repeated injury to the airway from chronic coughing in patients with COPD is the probable cause. These changes initially begin at the thoracic inlet but can progress to involve the entire intrathoracic trachea over time. Other smoking-related conditions may be present such as emphysema and respiratory bronchiolitis[49].

Tracheo-bronchomegaly

This is also referred to as Mounier-Kuhn syndrome. There is dilatation of the central airway with the mucosa projecting between the cartilaginous rings forming multiple diverticulae. This gives a characteristic corrugated appearance of trachea and mainstem bronchi (Figure 26). This entity is seen in patients with recurrent respiratory infections in their 3rd and 4th decade resulting in thinning of the muscularis mucosa of airway[50]. Mounier-Kuhn syndrome is characterized by tracheal diameter of more than 3 cm and mainstem bronchi diameters of greater than 2.4 cm[50,51].

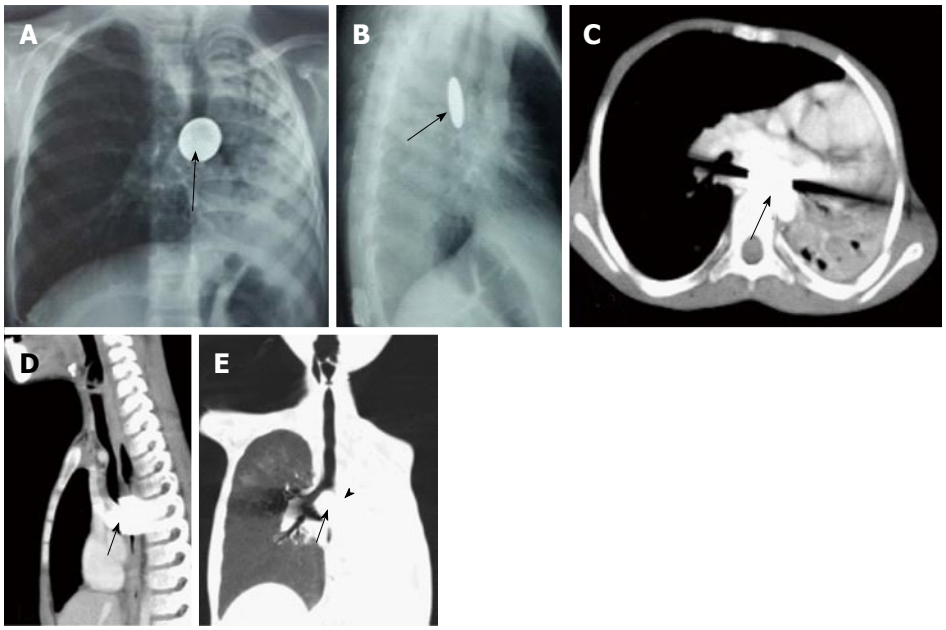

Figure 22 Impacted esophageal foreign body compressing airway. Frontal (A) and lateral (B) radiographs of chest reveal a well-defined round radio-opaque foreign body in the esophagus at the level of carina (arrows) with associated volume loss of left lung. Contrast enhanced axial (C) and sagittal (D) MPR images show a hyperdense foreign body giving streak artefacts impacted within the esophagus (arrow). Coronal MinIP image (E) shows near complete occlusion of left main bronchus (arrowhead) by the impacted esophageal foreign body (arrow) with collapse of left lung. MPR: Multiplanar reformation; MinIP: Minimum intensity projection.

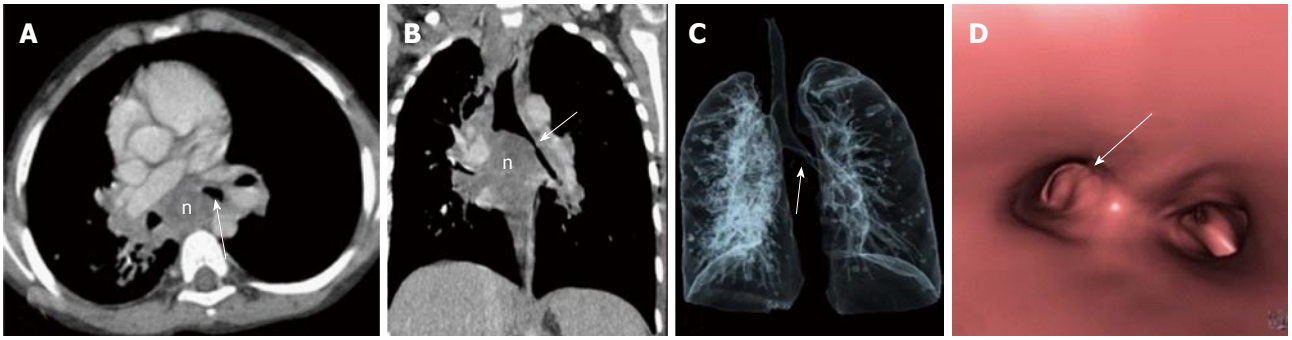

Figure 23 Enlarged tubercular lymph nodes compressing airway. Contrast enhanced axial (A) and coronal MPR (B) images show enlarged necrotic lymph nodal mass (n) in subcarinal station causing carinal widening and compression of left main bronchus (arrow). VRT (C) and virtual bronchoscopy (D) images also show compression of left main bronchus (arrow). MPR: Multiplanar reformation; VRT: Volume rendering technique.

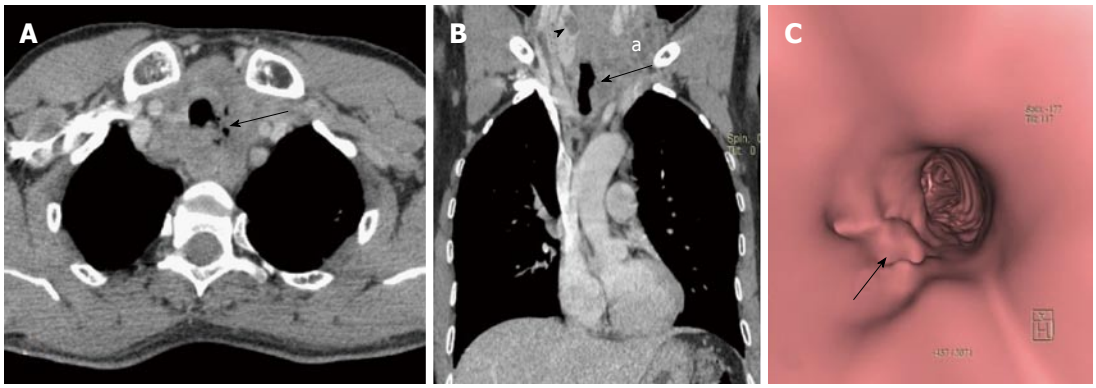

Figure 24 Paratracheal erosive malignant lymph nodes. Contrast enhanced axial (A) and coronal MPR (B) images show enlarged necrotic paratracheal lymph nodes eroding adjacent airway and showing foci of air within. There is a hypodense mass lesion (arrowhead in B) in right lobe of thyroid (patient was a known case of metastatic papillary thyroid carcinoma). Enlarged necrotic left lower jugular lymph nodes (a in B) also noted. Virtual bronchoscopy (C) shows focal area of irregularity along left lateral tracheal wall (arrow). MPR: Multiplanar reformation.

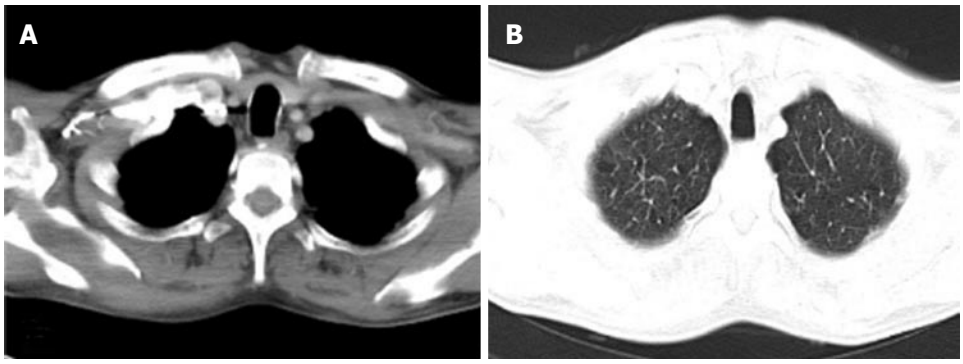

Figure 25 Saber-sheath trachea. In a 70-year old male with chronic obstructive pulmonary disease, axial images of thorax in mediastinal (A) and lung (B) window settings show increase in antero-posterior diameter of the trachea with narrowing of the transverse diameter. The sagittal to transverse diameter ratio measured 2.13:1.

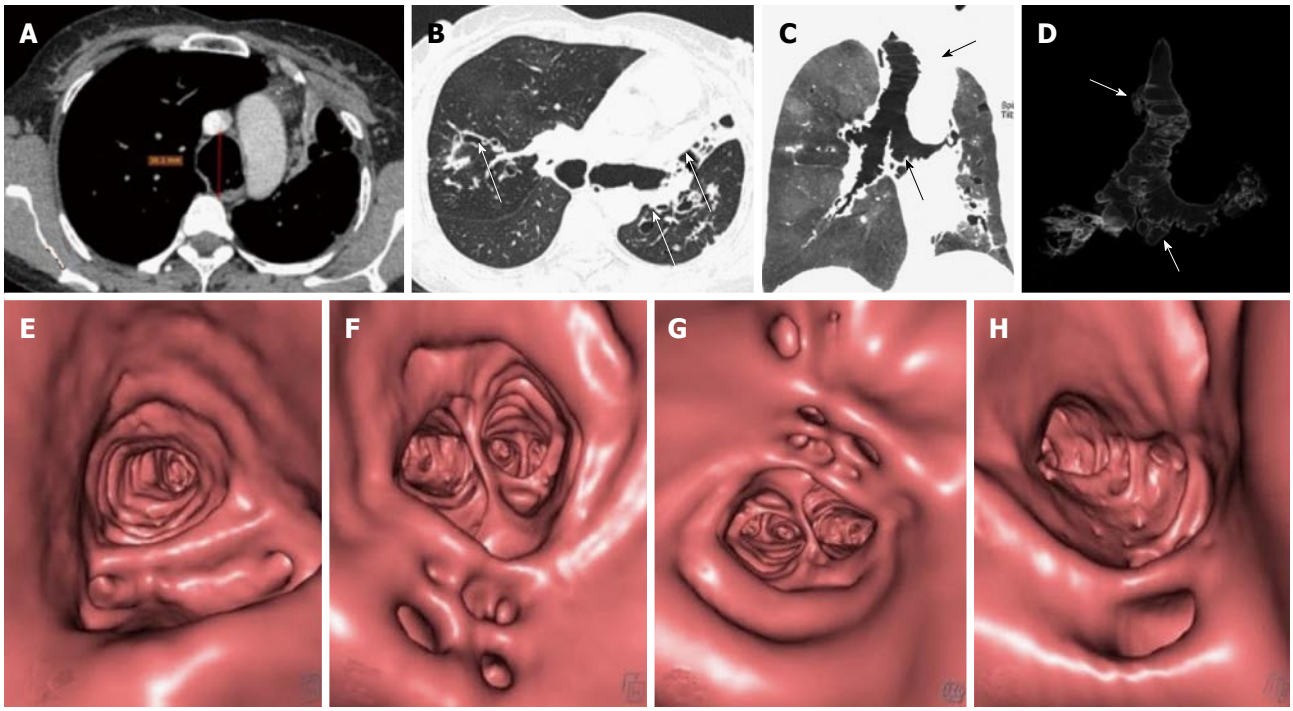

Figure 26 Mounier Kuhn syndrome. Axial images (A and B) show dilated trachea-AP diameter 3.6 cm at level of aortic arch (A) with dilated bronchi (B) and diverticula formation. Bronchiectasis is seen in bilateral upper and left lower lobes with collapse of lingula (arrow in B). Coronal MinIP (C) and VRT (D) images show tracheo-bronchomegaly with diffuse diverticulosis (arrows). Virtual bronchoscopy also shows diffusely scattered defects in the walls of upper trachea (E), carina (F), right (G) and left (H) main bronchi. MinIP: Minimum intensity projection; VRT: Volume rendering technique.

Tracheobronchopathia osteochondrodisplastica

Tracheobronchopathia osteochondroplastica is a rare, benign condition involving the trachea, and possibly major bronchi. The disease is characterised by diffuse nodularities, or polyps consisting of cartilaginous and/or osseous metaplastic tissue involving tracheal cartilagenous wall with sparing of membranous posterior wall (Figure 27)[52]. The nodules are 1 to 3 mm in diameter and may cause narrowing and rigidity of the trachea and bronchi. The majority of people remain asymptomatic throughout their lives unless severe airway stenosis develops, in which case patients may experience symptoms such as dyspnoea, hoarseness, persistent and often productive cough, haemoptysis and recurrent or slowly resolving pneumonia[53].

MISCELLANEOUS DEVELOPMENTAL ANOMALIES

Tracheal bronchus/displaced bronchus

The term tracheal bronchus was initially used for a right upper lobe bronchus originating from trachea by Sandifort in 1785. However, currently the term is applied for a variety of anomalous bronchi that supply the upper lobe or its apical segment. The anomalous bronchi may originate from trachea or main bronchi (Figure 28)[38]. Patients are usually asymptomatic. However, in patients presenting with persistent/recurrent pneumonia or atelectasis of the upper lobe, a possibility of tracheal bronchus should be kept in mind.

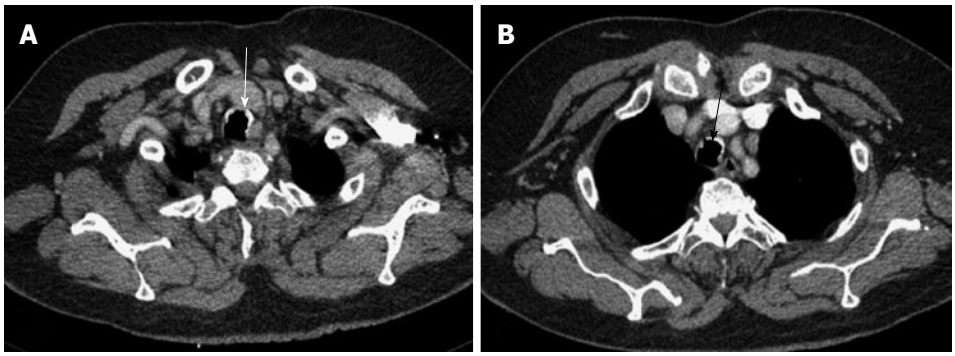

Figure 27 Tracheobronchopathia osteochondrodisplastica. Axial images of thorax (A and B) show irregular nodular thickening with foci of calcification involving the anterior and lateral walls of trachea (arrows). There is characteristic sparing of the posterior tracheal membrane.

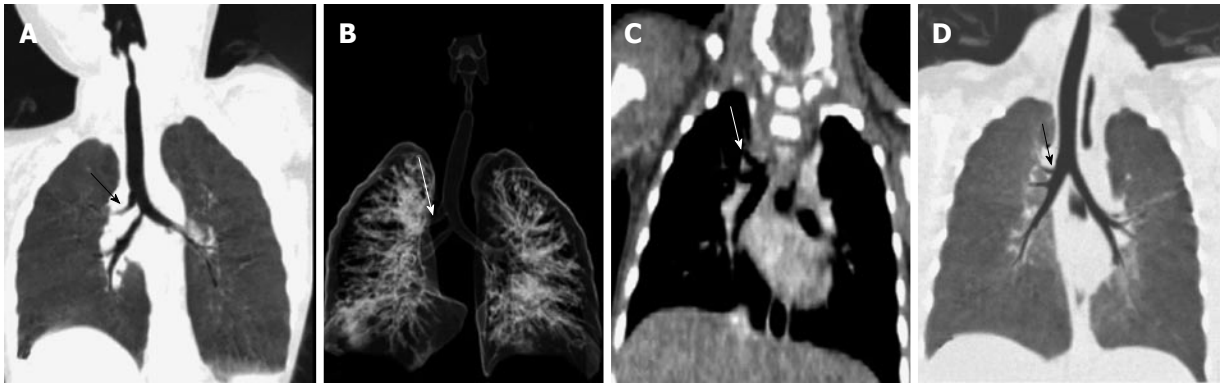

Figure 28 Displaced bronchus. Case 1: Coronal MinIP (A) and VRT (B) images show anomalous origin of right upper lobe bronchus from trachea-"Pig bronchus/bronchus suis" (arrow). Case 2: Coronal MPR (C) and MinIP (D) images show anomalous origin of the right apical segment bronchus from right main bronchus (arrow). MPR: Multiplanar reformation; MinIP: Minimum intensity projection; VRT: Volume rendering technique.

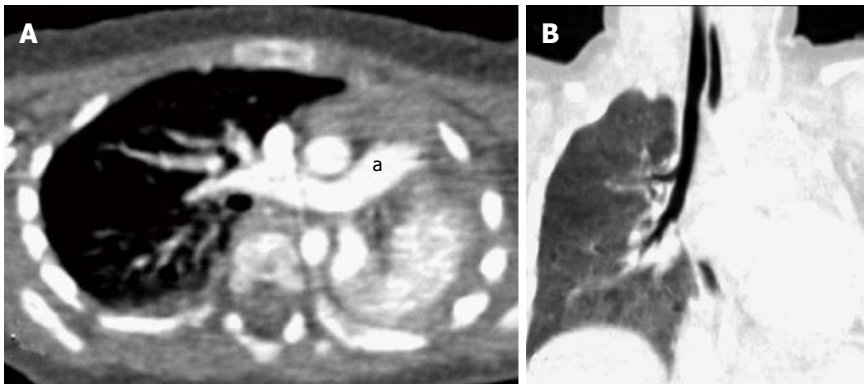

Figure 29 Bronchial agenesis. Axial (A) and coronal MinIP (B) images show absent left lung with left sided mediastinal shift and volume loss. Main pulmonary artery (a) continues as right pulmonary artery with absent left pulmonary artery. There is also associated absence of left main bronchus. MinIP: Minimum intensity projection.

Bronchial agenesis

Bronchial agenesis is always associated with congenital absence of lung, *i.e.*, pulmonary agenesis and absence of its vascular supply[54]. Bilateral lung agenesis is always fatal in antenatal or immediate postnatal period. Infants with unilateral agenesis usually survive, but they may have associated congenital heart disease, tracheaesophageal atresia, spinal and renal anomalies[39]. These neonates usually present with respiratory distress. They can also be discovered incidentally in older children and adults. MDCT is the modality of choice as it can easily diagnose the absence of lung parenchyma, bronchus and pulmonary vessels (Figure 29).

CONCLUSION

MDCT is a rapid and non-invasive investigation for evaluation of patients with suspected airway pathology. It is highly accurate in evaluating intraluminal obstruction, extraluminal vascular anomalies and airway wall

defects. The entire extra luminal anatomy anatomy is clearly delineated and any associated finding within the mediastinum or lung parenchyma is also clearly depicted. Therefore, it provides a comprehensive information about the extent of disease process including the luminal and extraluminal components. In addition, VB can also help access sites beyond a proximal stenosis which cannot be seen on conventional bronchoscopy due to the inability of bronchoscope to negotiate through a proximal occlusive lesion. Therefore MDCT has an immense potential to emerge as a non-invasive, rapidly reproducible investigation tool which can provide information about primary airway disease as well as extraluminal pathologies affecting the airway.

REFERENCES

1 **Burke AJ**, Vining DJ, McGuirt WF, Postma G, Browne JD. Evaluation of airway obstruction using virtual endoscopy. *Laryngoscope* 2000; **110**: 23-29 [PMID: 10646710 DOI: 10.1097/00005537-200001000-00005]

2 **Stern RL**, Cline HE, Johnson GA, Ravin CE. Three-dimensional imaging of the thoracic cavity. *Invest Radiol* 1989; **24**: 282-288 [PMID: 2745007 DOI: 10.1097/00004424-198904000-00005]

3 **Hu H**, He HD, Foley WD, Fox SH. Four multidetector-row helical CT: image quality and volume coverage speed. *Radiology* 2000; **215**: 55-62 [PMID: 10751468 DOI: 10.1148/radiology.215.1.r00ap3755]

4 **Rydberg J**, Buckwalter KA, Caldemeyer KS, Phillips MD, Conces DJ, Aisen AM, Persohn SA, Kopecky KK. Multisection CT: scanning techniques and clinical applications. *Radiographics* 2000; **20**: 1787-1806 [PMID: 11112829 DOI: 10.1148/radiographics.20.6.g00nv071787]

5 **Ravenel JG**, McAdams HP, Remy-Jardin M, Remy J. Multidimensional imaging of the thorax: practical applications. *J Thorac Imaging* 2001; **16**: 269-281 [PMID: 11685092 DOI: 10.1097/00005382-200110000-00008]

6 **Boiselle PM**, Reynolds KF, Ernst A. Multiplanar and three-dimensional imaging of the central airways with multidetector CT. *AJR Am J Roentgenol* 2002; **179**: 301-308 [PMID: 12130424 DOI: 10.2214/ajr.179.2.1790301]

7 **Remy-Jardin M**, Remy J, Artaud D, Fribourg M, Naili A. Tracheobronchial tree: assessment with volume rendering--technical aspects. *Radiology* 1998; **208**: 393-398 [PMID: 9680565 DOI: 10.1148/radiology.208.2.9680565]

8 **Higgins WE**, Ramaswamy K, Swift RD, McLennan G, Hoffman EA. Virtual bronchoscopy for three--dimensional pulmonary image assessment: state of the art and future needs. *Radiographics* 1998; **18**: 761-778 [PMID: 9599397 DOI: 10.1148/radiographics.18.3.9599397]

9 **Kay CL**, Evangelou HA. A review of the technical and clinical aspects of virtual endoscopy. *Endoscopy* 1996; **28**: 768-775 [PMID: 9007432 DOI: 10.1055/s-2007-1005603]

10 **Holbert JM**, Strollo DC. Imaging of the normal trachea. *J Thorac Imaging* 1995; **10**: 171-179 [PMID: 7674430 DOI: 10.1097/00005382-199522000-00003]

11 **Boiselle PM**, Lee KS, Ernst A. Multidetector CT of the central airways. *J Thorac Imaging* 2005; **20**: 186-195 [PMID: 16077334 DOI: 10.1097/01.rti.0000171624.84951.f2]

12 **Gamsu G**, Webb WR. Computed tomography of the trachea: normal and abnormal. *AJR Am J Roentgenol* 1982; **139**: 321-326 [PMID: 6979885 DOI: 10.2214/ajr.139.2.321]

13 **Naidich DP**, Webb WR. Introduction to imaging methodology and airway anatomy. In: Naidich DP, Webb WR, Grenier PA, Gefter WB, Harkin TJ, editor. Imaging of the Airways Functional and Radiologic Correlations. Philadelphia: Lippincott Williams and Wilkins, 2005: 1-28

14 **Ngo AV**, Walker CM, Chung JH, Takasugi JE, Stern EJ, Kanne JP, Reddy GP, Godwin JD. Tumors and tumorlike conditions of the large airways. *AJR Am J Roentgenol* 2013; **201**: 301-313 [PMID: 23883210 DOI: 10.2214/AJR.12.9043]

15 **Jemal A**, Siegel R, Xu J, Ward E. Cancer statistics, 2010. *CA Cancer J Clin* 2010; **60**: 277-300 [PMID: 20610543 DOI: 10.3322/caac.20073]

16 **Hartman TE**, Tazelaar HD, Swensen SJ, Müller NL. Cigarette smoking: CT and pathologic findings of associated pulmonary diseases. *Radiographics* 1997; **17**: 377-390 [PMID: 9084079 DOI: 10.1148/radiographics.17.2.9084079]

17 **Travis WD**. Pathology of lung cancer. *Clin Chest Med* 2002; **23**: 65-81, viii [PMID: 11901921 DOI: 10.1016/S0272-5231(03)00061-3]

18 **Pearlberg JL**, Sandler MA, Lewis JW, Beute GH, Alpern MB. Small-cell bronchogenic carcinoma: CT evaluation. *AJR Am J Roentgenol* 1988; **150**: 265-268 [PMID: 2827450 DOI: 10.2214/ajr.150.2.265]

19 **Rady PL**, Schnadig VJ, Weiss RL, Hughes TK, Tyring SK. Malignant transformation of recurrent respiratory papillomatosis associated with integrated human papillomavirus type 11 DNA and mutation of p53. *Laryngoscope* 1998; **108**: 735-740 [PMID: 9591556 DOI: 10.1097/00005537-199805000-00021]

20 **Park CM**, Goo JM, Lee HJ, Kim MA, Lee CH, Kang MJ. Tumors in the tracheobronchial tree: CT and FDG PET features. *Radiographics* 2009; **29**: 55-71 [PMID: 19168836 DOI: 10.1148/rg.291085126]

21 **Jeong SY**, Lee KS, Han J, Kim BT, Kim TS, Shim YM, Kim J. Integrated PET/CT of salivary gland type carcinoma of the lung in 12 patients. *AJR Am J Roentgenol* 2007; **189**: 1407-1413 [PMID: 18029878 DOI: 10.2214/AJR.07.2652]

22 **Hartman TE**, Primack SL, Lee KS, Swensen SJ, Müller NL. CT of bronchial and bronchiolar diseases. *Radiographics* 1994; **14**: 991-1003 [PMID: 7991828 DOI: 10.1148/radiographics.14.5.7991828]

23 **Gustafsson BI**, Kidd M, Chan A, Malfertheiner MV, Modlin IM. Bronchopulmonary neuroendocrine tumors. *Cancer* 2008; **113**: 5-21 [PMID: 18473355 DOI: 10.1002/cncr.23542]

24 **Marom EM**, Goodman PC, McAdams HP. Focal abnormalities of the trachea and main bronchi. *AJR Am J Roentgenol* 2001; **176**: 707-711 [PMID: 11222209 DOI: 10.2214/ajr.176.3.1760707]

25 **Chang CH**, Wang HC, Wu MT, Lu JY. Virtual bronchoscopy for diagnosis of recurrent respiratory papillomatosis. *J Formos Med Assoc* 2006; **105**: 508-511 [PMID: 16801040]

26 **Kozower BD**, Javiden-Nejad C, Lewis JS, Safdar S, Cooper JD, Patterson GA. Clinical-pathologic conference in general thoracic surgery: malignant transformation of recurrent respiratory papillomatosis. *J Thorac Cardiovasc Surg* 2005; **130**: 1190-1193 [PMID: 16214538 DOI: 10.1016/j.jtcvs.2005.06.036]

27 **Taha MS**, Mostafa BE, Fahmy M, Ghaffar MK, Ghany EA. Spiral CT virtual bronchoscopy with multiplanar reformatting in the evaluation of post-intubation tracheal stenosis: comparison between endoscopic, radiological and surgical findings. *Eur Arch Otorhinolaryngol* 2009; **266**: 863-866 [PMID: 19002699 DOI: 10.1007/s00405-008-0854-y]

28 **Lee KS**, Yoon JH, Kim TK, Kim JS, Chung MP, Kwon OJ. Evaluation of tracheobronchial disease with helical CT with multiplanar and three-dimensional reconstruction: correlation with bronchoscopy. *Radiographics* 1997; **17**: 555-567; discussion 568-570 [PMID: 9153696 DOI: 10.1148/radiographics.17.3.9153696]

29 **Koşucu P**, Ahmetoğlu A, Koramaz I, Orhan F, Ozdemir O, Dinç H, Okten A, Gümele HR. Low-dose MDCT and virtual bronchoscopy in pediatric patients with foreign body aspiration. *AJR Am J Roentgenol* 2004; **183**: 1771-1777 [PMID: 15547227 DOI: 10.2214/ajr.183.6.01831771]

30 **Applegate KE**, Dardinger JT, Lieber ML, Herts BR, Davros WJ, Obuchowski NA, Maneker A. Spiral CT scanning technique in the detection of aspiration of LEGO foreign bodies. *Pediatr Radiol* 2001; **31**: 836-840 [PMID: 11727016 DOI: 10.1007/s002470100001]

31 **Karakoç F**, Karadağ B, Akbenlioğlu C, Ersu R, Yildizeli B, Yüksel

M, Dağli E. Foreign body aspiration: what is the outcome? *Pediatr Pulmonol* 2002; **34**: 30-36 [PMID: 12112794 DOI: 10.1002/ppul.10094]
32 **Khan MF**, Herzog C, Ackermann H, Wagner TO, Maataoui A, Harth M, Abolmaali ND, Jacobi V, Vogl TJ. Virtual endoscopy of the tracheo-bronchial system: sub-millimeter collimation with the 16-row multidetector scanner. *Eur Radiol* 2004; **14**: 1400-1405 [PMID: 15133710 DOI: 10.1007/s00330-004-2325-1]
33 **Slim MS**, Yacoubian HD. Complications of foreign bodies in the tracheobronchial tree. *Arch Surg* 1966; **92**: 388-393 [PMID: 5906833 DOI: 10.1001/archsurg.1966.01320210068013]
34 **Zerella JT**, Dimler M, McGill LC, Pippus KJ. Foreign body aspiration in children: value of radiography and complications of bronchoscopy. *J Pediatr Surg* 1998; **33**: 1651-1654 [PMID: 9856887 DOI: 10.1016/S0022-3468(98)90601-7]
35 **Seo JB**, Song KS, Lee JS, Goo JM, Kim HY, Song JW, Lee IS, Lim TH. Broncholithiasis: review of the causes with radiologic-pathologic correlation. *Radiographics* 2002; **22** Spec No: S199-S213 [PMID: 12376611 DOI: 10.1148/radiographics.22.suppl_1.g02oc07s199]
36 **Moriwaki Y**, Sugiyama M, Matsuda G, Toyoda H, Kosuge T, Uchida K, Fukuyama H, Iwashita M, Morimura N, Suzuki J, Yamamoto T, Suzuki N. Usefulness of the 3-dimensionally reconstructed computed tomography imaging for diagnosis of the site of tracheal injury (3D-tracheography). *World J Surg* 2005; **29**: 102-105 [PMID: 15599743 DOI: 10.1007/s00268-004-7433-1]
37 **Turner A**, Gavel G, Coutts J. Vascular rings--presentation, investigation and outcome. *Eur J Pediatr* 2005; **164**: 266-270 [PMID: 15666159 DOI: 10.1007/s00431-004-1607-6]
38 **Berrocal T**, Madrid C, Novo S, Gutiérrez J, Arjonilla A, Gómez-León N. Congenital anomalies of the tracheobronchial tree, lung, and mediastinum: embryology, radiology, and pathology. *Radiographics* 2004; **24**: e17 [PMID: 14610245 DOI: 10.1148/rg.e17]
39 **Lee EY**, Boiselle PM, Cleveland RH. Multidetector CT evaluation of congenital lung anomalies. *Radiology* 2008; **247**: 632-648 [PMID: 18487532 DOI: 10.1148/radiol.2473062124]
40 **Kimura-Hayama ET**, Meléndez G, Mendizábal AL, Meave-González A, Zambrana GF, Corona-Villalobos CP. Uncommon congenital and acquired aortic diseases: role of multidetector CT angiography. *Radiographics* 2010; **30**: 79-98 [PMID: 20083587 DOI: 10.1148/rg.301095061]
41 **Schanker HM**, Rachelefsky G, Siegel S, Katz R, Spector S, Rohr A, Rodriquiz C, Woloshin K, Papanek PJ. Immediate and delayed type hypersensitivity to malathion. *Ann Allergy* 1992; **69**: 526-528 [PMID: 1471787]
42 **Aktoğu S**, Yuncu G, Halilçolar H, Ermete S, Buduneli T. Bronchogenic cysts: clinicopathological presentation and treatment. *Eur Respir J* 1996; **9**: 2017-2021 [PMID: 8902460 DOI: 10.1183/09031936.96.09102017]
43 **McAdams HP**, Kirejczyk WM, Rosado-de-Christenson ML, Matsumoto S. Bronchogenic cyst: imaging features with clinical and histopathologic correlation. *Radiology* 2000; **217**: 441-446 [PMID: 11058643 DOI: 10.1148/radiology.217.2.r00nv19441]
44 **Williams HJ**, Johnson KJ. Imaging of congenital cystic lung lesions. *Paediatr Respir Rev* 2002; **3**: 120-127 [PMID: 12297058 DOI: 10.1016/S1526-0550(02)00006-9]
45 **Torres de Amorim e Silva CJ**, Fink AM. Case 137: Pneumonia and bronchiectasis secondary to unrecognized peanut impaction. *Radiology* 2008; **248**: 1080-1082 [PMID: 18710997 DOI: 10.1148/radiol.2483050725]
46 **Urkin J**, Bar-David Y. Respiratory distress secondary to esophageal foreign body: a case report. *ScientificWorldJournal* 2006; **6**: 16-19 [PMID: 16432624 DOI: 10.1100/tsw.2006.08]
47 **Edlavitch SA**, Crow R, Burke GL, Huber J, Prineas R, Blackburn H. The effect of the number of electrocardiograms analyzed on cardiovascular disease surveillance: the Minnesota Heart Survey (MHS). *J Clin Epidemiol* 1990; **43**: 93-99 [PMID: 2319286 DOI: 10.1002/ppul.22728]
48 **Grenier PA**, Beigelman-Aubry C, Brillet PY. Nonneoplastic tracheal and bronchial stenoses. *Radiol Clin North Am* 2009; **47**: 243-260 [PMID: 19249454 DOI: 10.1016/j.rcl.2008.11.011]
49 **Trigaux JP**, Hermes G, Dubois P, Van Beers B, Delaunois L, Jamart J. CT of saber-sheath trachea. Correlation with clinical, chest radiographic and functional findings. *Acta Radiol* 1994; **35**: 247-250 [PMID: 8192961 DOI: 10.1177/028418519403500310]
50 **Shin MS**, Jackson RM, Ho KJ. Tracheobronchomegaly (Mounier-Kuhn syndrome): CT diagnosis. *AJR Am J Roentgenol* 1988; **150**: 777-779 [PMID: 3258088 DOI: 10.2214/ajr.150.4.777]
51 **Jain P**, Dave M, Singh DP, Kumawat DC, Babel CS. Mounier-Kuhn syndrome. *Indian J Chest Dis Allied Sci* 2002; **44**: 195-198 [PMID: 12206481]
52 **Chroneou A**, Zias N, Gonzalez AV, Beamis JF. Tracheobronchopathia osteochondroplastica. An underrecognized entity? *Monaldi Arch Chest Dis* 2008; **69**: 65-69 [PMID: 18837419]
53 **Zack JR**, Rozenshtein A. Tracheobronchopathia osteochondroplastica: report of three cases. *J Comput Assist Tomogr* 2002; **26**: 33-36 [PMID: 11801902 DOI: 10.1097/00004728-200201000-00006]
54 **Ghaye B**, Szapiro D, Fanchamps JM, Dondelinger RF. Congenital bronchial abnormalities revisited. *Radiographics* 2001; **21**: 105-119 [PMID: 11158647 DOI: 10.1148/radiographics.21.1.g01ja06105]

P- Reviewer: Chow J, Yazdi HR **S- Editor**: Gong ZM **L- Editor**: A **E- Editor**: Wu HL

Published by **Baishideng Publishing Group Inc**
8226 Regency Drive, Pleasanton, CA 94588, USA
Telephone: +1-925-223-8242
Fax: +1-925-223-8243
E-mail: bpgoffice@wjgnet.com
Help Desk: http://www.wjgnet.com/esps/helpdesk.aspx
http://www.wjgnet.com